

Automatic Segmentation of Short-Axis Cardiac MRI Using a Biventricular Deformable Model with an Explicit Thickness Prior

P. A. Yushkevich¹, H. Sun¹, F. M. Sukno², C. Tobon-Gomez², H. Wang¹, and A. F. Frangi²

¹PICSL, Department of Radiology, University of Pennsylvania, Philadelphia, PA, United States, ²CISTIB, Universitat Pompeu Fabra, CIBER-BBN, Barcelona, Spain

Purpose: Accurate segmentation of the myocardium is often a prerequisite for quantitative analysis of short-axis cardiac MRI. Automatic myocardium segmentation is challenging due to the limitations of image resolution and to complex anatomy. Right ventricle (RV) segmentation is particularly difficult because the RV wall is very thin relative to the typical voxel size. Most existing methods only segment the epicardium or the endocardium of the RV, or do not segment the RV at all. We hypothesize that a statistical shape model of the myocardium with an explicit specification of thickness and thickness variability can be used to reliably segment both the endocardial and the epicardial surface in both ventricles. To test this hypothesis, we develop and evaluate an approach that models the myocardium using a *deformable medial model* (a geometric model specified in terms of the medial axis and thickness rather than, say, boundary) and uses a Markov prior to model thickness variability.

Methods: Deformable Medial Model. A triangle mesh consisting of three manifolds (roughly corresponding to the LV wall, RV wall, and interventricular septum) is used to model the medial axis of the myocardium (Fig. 1a). At each vertex in the mesh, a scalar thickness value is specified. From the medial axis and thickness scalar field, a volumetric model of the myocardium is derived, such that the medial axis transform of the boundary of the volumetric model is identical to that specified in the medial model. This transformation, known as *inverse skeletonization*, has been studied in our earlier work [1]. Statistical Shape and Thickness Priors. The deformable medial model is fitted to binary segmentations of the myocardium on a training set of 81 end-diastole images in order to construct a statistical shape and thickness prior. Fitting involves maximizing the overlap between the derived volumetric model and the binary segmentation (Fig. 1b-d). The statistical shape prior is constructed by modeling variability in the vertices of the medial axis mesh using PCA (similar to Active Shape Models [2]) and modeling thickness at the vertices as a Markov random field. MRI Segmentation. Deformable medial models are fitted to MRI data by minimizing a Bayesian objective function. The prior component of the objective is computed using the shape and thickness priors above. The likelihood component is computed by searching for new candidate position of each vertex in the medial model using a local statistical model of appearance derived from the training data. Additional energy terms ensure that the medial model satisfies necessary geometrical constraints in [1]. The segmentation is manually initialized by placing six landmarks in the MR volume. Evaluation Dataset. The method is evaluated in short-axis cardiac MRI of patients with myocardial infarction (MI, n=10), hypertrophic cardiomyopathy (HCM, n=10), dilated cardiomyopathy (DCM, n=10), and normal subjects (NOR, n=10). Short-axis cine MRI was acquired on a GE Signa CVi-HDx 1.5T scanner with a dedicated cardiac coil (multi-slice bSSFP sequence, TR/TE=2.9/1.2 ms, FA=45°, NEX=1, 1.56 mm × 1.56 mm × 8 mm voxels, 30 cardiac phases). The myocardium was manually segmented in end diastole images by H.S. The images were partitioned into training (n=24) and test (n=16) subsets, with the training subset used to build the appearance model and the test set used to evaluate the segmentation of end-diastole images. The experiment was repeated 10 times with random repartitioning.

Results: Figure 2 gives an example of automatic segmentation. The average point-to-surface distances between automatic and manual segmentations are listed for different cohorts and anatomical regions in Table 1. Adding Gaussian noise with $\sigma=5$ to the coordinates of the landmarks used for initialization reduces these distances by only about 5%. The average Dice overlap between automatic and manual segmentations is 0.86 ± 0.03 (NOR: 0.85 ± 0.02 ; MI: 0.86 ± 0.04 ; DCM: 0.86 ± 0.02 ; HCM: 0.88 ± 0.02). LV and RV volumes derived from the automatic segmentation are similar to the volumes derived from the manual segmentation: for the LV, the average bias is -2.56 ± 3.62 ml and the coefficient of variance (CoV) is 3.42%. For the RV, the average bias is -7.52 ± 4.55 ml and the CoV is 5.28%.

Discussion: Automatic segmentation results are highly consistent with manual segmentations. Our results are highly competitive with segmentation results reported in the literature, as shown in Table 2. The agreement between automatically and manually derived LV and RV volumes is well in range of inter-observer reliability of manual volume estimation reported in the literature [3]. Unlike most techniques, our method generates both the epicardial and endocardial surface of the RV. An estimate of myocardial thickness is provided “for free” by the method, since thickness forms part of the deformable model specification. This makes the method particularly applicable to automatic assessment of pathologies affecting heart wall thickness. Future work involves extending the method to multiple time points.

References: [1] Yushkevich et al., IEEE-TMI 25:2:1547–64 (2006); [2] Cootes et al., CVIU 61:1:38-59 (1995); [3] Luijnenburg et al., Int J Cardiovasc Imaging 26:1:57-64 (2010); [4] Mitchell et al., IEEE-TMI 21:9:1167-78 (2002); [5] Kaus et al., Med Image Anal 8:3:245–54 (2004); [6] Lotjonen et al., Med Image Anal 8:3: 371–86 (2004); [7] Tölli et al., MICCAI 2006; [8] van Assen et al., IEEE TITB 12:5:595–605 (2008); [9] Zhuang et al., MICCAI 2008; [10] Jolly et al., MICCAI 2009; [11] Peters et al., Med Image Anal 14:1:70–84 (2010).

Acknowledgements: P.Y. and H.W. are supported by NIH grants AG027785 and NS061111. A.F, F.S. and C.T.G. are supported by grants CDTI CENIT- CDTEAM, CENIT-cvREMOD, TIN2009-14536-C02-01 from the Spanish Ministry of Science and Innovation and the European Commission grant euHeart (FP7-ICT-224495).

Table 1. Mean surface distance between automatic and manual segmentations.

	LV (mm)	RV (mm)	EPI (mm)	All (mm)
NOR	0.78 ± 0.13	1.07 ± 0.20	0.96 ± 0.20	0.94 ± 0.14
MI	0.94 ± 0.37	1.16 ± 0.34	1.06 ± 0.38	1.05 ± 0.36
DCM	0.88 ± 0.19	1.33 ± 0.29	0.97 ± 0.13	1.03 ± 0.12
HCM	0.87 ± 0.15	1.19 ± 0.22	0.92 ± 0.12	0.97 ± 0.10

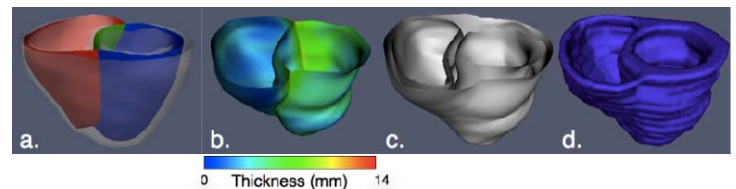


Figure 1. Illustration of medial models. (a) The template medial model, showing the three surfaces forming the myocardium skeleton. (b). Template deformed to fit the binary segmentation in (d), with color indicating thickness. (c) epicardial/endocardial surfaces of the model in (b). (d). Binary segmentation.

Table 2. Comparison with published results.

Method	Resolution (mm ³)	LV (mm)	RV (mm)	EPI (mm)
Mitchell '02 [4] ^{p,c}	$1.56 \times 1.56 \times 9$	$2.75 \pm 0.86^*$	-	$2.63 \pm 0.76^\dagger$
Kaus '04 [5] ^{p,c}	$1.25 \times 1.25 \times 10$	2.28 ± 0.93	-	$2.62 \pm 0.75^\dagger$
Lotjonen '04 [6] ^c	$1.0 \times 1.0 \times \text{var.}^{**}$	2.01 ± 0.31	2.37 ± 0.50	$2.77 \pm 0.49^\dagger$
Tölli '06 [7] ^c	$1.0 \times 1.0 \times \text{var.}^{**}$	1.77 ± 0.36	2.13 ± 0.63	$1.85 \pm 0.51^\dagger$
van Assen '08 [8] ^c	$1.5 \times 1.5 \times 10$	1.72	-	1.55^\dagger
Zhuang '08 [9] ^c	$2 \times 2 \times 2$	2.4 ± 1.1	2.6 ± 1.5	$1.3 \pm 0.21^\dagger$
Jolly [10] ⁰⁹	$1.25 \times 1.25 \times 8$	2.26	-	1.97^\dagger
Peters '10 [11] ^p	$0.6 \times 0.6 \times 0.8$	0.69 ^{***}	0.74	0.83^\dagger
Our method ^{p,c}	$1.56 \times 1.56 \times 8$	0.87 ± 0.23	1.19 ± 0.28	$0.98 \pm 0.23^\dagger$

^p Evaluation in patients. ^c Evaluation in controls. ^{*} Distance measured in 2D. ^{**} Short and long axis slices. ^{***} Error measured as surface to surface distance. [†] LV epicardium only. [‡] LV+RV epicardium.

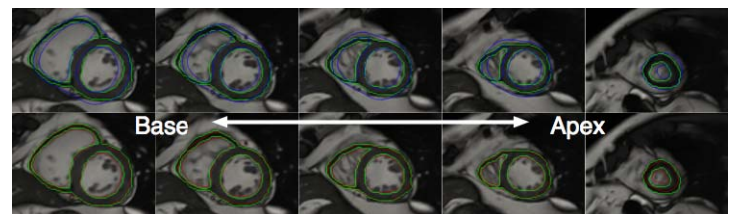


Figure 2. Segmentation example. Top row: initial model placement (blue) vs. manual segmentation (green). Bottom row: final segmentation (red) vs. manual (green).